
EFDA-JET-CP(06)02-09

T. Eich, A. Kallenbach, S. Jachmich, P.L. Andrew, J.C. Fuchs, W. Fundamenski,
A.Herrmann, R.A. Pitts, J.Neuhauser, ASDEX Upgrade Team
and JET EFDA contributors

Divertor Power Deposition and Target Current Asymmetries during Type-I ELMs in JET and ASDEX Upgrade

“This document is intended for publication in the open literature. It is made available on the understanding that it may not be further circulated and extracts or references may not be published prior to publication of the original when applicable, or without the consent of the Publications Officer, EFDA, Culham Science Centre, Abingdon, Oxon, OX14 3DB, UK.”

“Enquiries about Copyright and reproduction should be addressed to the Publications Officer, EFDA, Culham Science Centre, Abingdon, Oxon, OX14 3DB, UK.”

Divertor Power Deposition and Target Current Asymmetries during Type-I ELMs in JET and ASDEX Upgrade

T. Eich¹, A. Kallenbach¹, S. Jachmich², P.L. Andrew³, J.C. Fuchs¹, W. Fundamenski³,
A. Herrmann¹, R.A. Pitts⁴, J. Neuhauser¹, ASDEX Upgrade Team
and JET EFDA contributors*

¹*Institut für Plasmaphysik, Forschungszentrum Jülich GmbH, EURATOM Association,
Trilateral Euregio Cluster, D-52425 Jülich, Germany*

²*Max-Planck-Institut für Plasmaphysik, EURATOM Association, 85748 Garching, Germany*

³*EURATOM/UKAEA Fusion Association, Culham Science Centre, Abingdon, OX14 3DB, UK*

⁴*FOM-Instituut voor Plasmafysica, Nieuwegein, The Netherlands*

⁵*EFDA Close Support Unit – Garching, Boltzmannstrasse 2, D-85748 Garching, Germany*

* See annex of J. Pamela et al, "Overview of JET Results",

(Proc. \square^{th} IAEA Fusion Energy Conference, Vilamoura, Portugal (2004).

ABSTRACT

Analysis of the type-I ELM power load asymmetries using infra-red thermography and target current measurements is performed in JET DOC-L and ASDEX Upgrade Upper Single Null type-I ELMy H-Mode discharges with ‘normal’ and ‘reversed’ field direction, i.e. with the ion $B \times \nabla B$ drift direction pointing towards the active X-point and the ion $B \times \nabla B$ drift direction pointing away from the active X-point, respectively. The ELM power load towards the inner target plate is found to be larger as towards the outer target with ‘normal’ field direction and vice versa with ‘reversed’ field. Current measurements are performed in ASDEX Upgrade providing information that the inner target receives a net positive and the outer target a net negative charge during the ELM in ‘normal’ field and vice versa for discharges with ‘reversed’ field. The difference between the ELM energy load on the inner and outer target, $E_{\text{outer}} - E_{\text{inner}}$, is well correlated with the net charge due to the ‘ELM giving a net charge of 5As for a value of 5kJ for $E_{\text{outer}} - E_{\text{inner}}$. A comparison to JET data shows that in both devices the maximum difference for values on $E_{\text{outer}} - E_{\text{inner}}$ for ‘normal’ field direction, as foreseen in ITER, corresponds to values of $E_{\text{outer}} - E_{\text{inner}} = 2$.

1. INTRODUCTION AND EXPERIMENTAL DATA BASE

The target power deposition during edge localized modes [1] (ELMs) is a concern for the divertor target plates [2,3] in ITER. For an extrapolation of target power load characteristics (measured by infra-red thermography) of present devices such as ASDEX Upgrade and JET to ITER it is necessary to understand the ELM related SOL transport physics. For this reason, in JET and ASDEX Upgrade dedicated discharges for optimized infra-red measurements have been performed, complemented by target integrated current measurements in ASDEX Upgrade [4] and probe measurements in JET [5]. To study the effect of ELM loss size, pedestal temperature and density and particle drifts on type-I ELM SOL transport, experiments were performed with varying heating power, plasma density and field direction. The field direction with the ion $B \times \nabla B$ drift direction pointing towards the active X-point will be named as ‘normal’ throughout the paper, and the ion $B \times \nabla B$ drift direction pointing away from the X-point as ‘reversed’. It should be noted that the field direction change in ASDEX Upgrade is achieved by switching only the toroidal magnetic field whereas in JET both the direction of the toroidal magnetic field and the toroidal plasma current direction are switched.

Although progress was made for quantifying the ELM target load characteristics as expected for ITER [6], the underlying transport mechanism driving a larger fraction of the ELM released energy towards the inner target plates than to the outer in ‘normal’ field direction [7] is still not resolved. Therefore, this paper focuses on the latter issue and presents correlation of the ELM target deposited energy asymmetries with net target charge due to ELMs. Co-deposited surface layers can influence the correct estimation of power fluxes from surface temperature measurements [7]. These layers are reported from JET [8] to be deposited largely asymmetrically on the inner and outer target tiles depending on the field direction. Therefore such influences have been minimized in ASDEX Upgrade upper single null discharges by installing new and therefore clean target tiles (for details see [9]). All

presented data are obtained by using coherent averaging techniques, in which about at least 10-20 ELMs are used for one data point in this work.

2. POWER DEPOSITION AND TARGET CURRENTS DURING TYPE-I ELMs

Before the ELM induced target power and target current are presented, the corresponding value for the Inter-ELM transport should be briefly discussed for both field directions. In the Inter-ELM phases with ‘normal’ field, generally at target thermo current is observed caused by the difference of the local electron temperature, T_e , at the target plates with T_e being reported to be larger at the outer target [10, 4]. Also commonly observed, a larger fraction of the Inter-ELM released power into the SOL is deposited on the outer divertor target plates due to the ballooning-like nature of tokamak energy release from the confined plasma into the SOL, which causes poloidally localized power outward fluxes at the outer equatorial midplane [7]; this ballooning-like power release is reported not to change during the ELM energy release, see e.g. [11]. In ‘reversed’ field cases, the Inter-ELM target power deposition is reported to be roughly equal and no change of the midplane power release origin is observed. Measured thermo currents change flow direction for ‘reversed’ field interpreted as a larger T_e at the inner target for that case.

Figure 1 (a) shows the experimental set up for the power flux and target current measurements in ASDEX Upgrade upper single null discharges for ‘normal’ field direction. Figure 1(b) shows that during the ELM a larger fraction of the ELM induced power is deposited on the inner target than on the outer (inversing to the Inter-ELM ratio) and simultaneously that the observed target current is increased but keeping the same flow direction as in the Inter-ELM phase. Figure 1(c) shows the time integrals of the values presented in (b) giving the ELM energy for inner, E_{inner} , and outer target, E_{outer} , and the ELM related charge difference, C_{ELM} , between both target plates; Note that C_{ELM} is negative in the latter case, i.e. a negative current flows from the inner to the outer target plate through the SOL during the ELM. Since the poloidal origin of the energy release location has not significantly changed from the Inter-ELM to the ELM phase, it may surprise that a larger fraction of the ELM energy is deposited onto the inner divertor target.

Figure 2 shows the same quantities as in Figure 1 for a similar discharge in ASDEX Upgrade with ‘reversed’ field. Here, a situation is observed with a larger value for E_{outer} than for E_{inner} and simultaneously a positive value for C_{ELM} .

Summarizing these findings a higher energy load is observed on that target plate, which receives a net positive charge. A net negative charge of same absolute size within the error bars is measured for the target with the lower ELM energy load. Consequently, the target with lower value for T_e in the Inter-ELM phases (and also during the ELM) receives the larger power load during the ELM independently on the field direction.

3. CORRELATION OF ELM TARGET ENERGY WITH TARGET CHARGE

Figure 3 shows the correlation between the difference of ELM target load for outer and inner target, -

$E_{\text{outer}} - E_{\text{inner}}$, and the ELM related net charge C_{ELM} with the convention

$$C_{\text{ELM}} = C_{\text{ele}}^{\text{inner}} - C_{\text{ion}}^{\text{inner}} = C_{\text{ion}}^{\text{outer}} - C_{\text{ele}}^{\text{outer}}.$$

As it is obvious from the plot, both quantities are well correlated. Different aspects of the correlation should be noted by the reader. First, both quantities strictly change sign with field direction. Secondly, the graph passes through zero for $E_{\text{outer}} - E_{\text{inner}} = 0$, i.e. for a balanced ELM target power load no ELM related currents are measured. Finally, the gradient of the graph for, ‘normal’ and ‘reversed’ field are different roughly by a factor or two. By focusing in the following analysis on the ‘normal’ field direction the ratio between energy and net charge difference is revealed from the gradient of the graph in Figure 4 with

$$\frac{E_{\text{outer}} - E_{\text{inner}}}{C_{\text{ELM}}} = \frac{-5\text{kJ}}{-5\text{As}}.$$

In the following two cases are discussed, first (1) a case where the net charge difference is fully attributed to electron flows (thermo currents) and secondly (2) where the net charge difference is fully attributed to the ions.

- (1) Thermo currents [12,13] are observed in ASDEX Upgrade for ‘normal’ field direction to cause in Inter-ELM phases a larger T_e at the outer target than at the inner [4]. Since the target currents only increase in amplitude but otherwise do not change the sign (see Figure 1 and Figure 2 and Figure 1 in [4]), thermo currents cannot be responsible to explain the measured change of ELM energy load being larger at inner target.
- (2) In the next step the measured net charge at the targets plates is fully attributed to ions, i.e.

$$C_{\text{ELM}} = -C_{\text{ion}}^{\text{inner}} - C_{\text{ion}}^{\text{outer}} \text{ and } C_{\text{ele}}^{\text{inner}} = -C_{\text{ele}}^{\text{outer}} = 0.$$

The ELM energy load for each target is explicitly expressed by numbers of ions and electrons

$$E_{\text{outer}} = \gamma_{\text{ion}}^{\text{outer}} k_B T_{\text{ion}}^{\text{outer}} (N_{\text{ELM}}^{\text{outer}} + C_{\text{ion}}^{\text{outer}}) + \gamma_{\text{ele}}^{\text{outer}} k_B T_{\text{ele}}^{\text{outer}} (N_{\text{ELM}}^{\text{outer}} + C_{\text{ion}}^{\text{outer}})$$

$$E_{\text{inner}} = \gamma_{\text{ion}}^{\text{inner}} k_B T_{\text{ion}}^{\text{inner}} (N_{\text{ELM}}^{\text{inner}} + C_{\text{ion}}^{\text{inner}}) + \gamma_{\text{ele}}^{\text{inner}} k_B T_{\text{ele}}^{\text{inner}} (N_{\text{ELM}}^{\text{inner}} + C_{\text{ion}}^{\text{inner}})$$

With $N_{\text{ELM}}^{\text{outer}}$, $N_{\text{ELM}}^{\text{inner}}$ being the number of pairs of electrons and ions (and therefore not causing a charge difference) deposited in the outer and inner, respectively. Unfortunately no probe measurements have been available for the presented upper single null discharges in ASDEX Upgrade and therefore a variety of assumptions have to be made, i.e.

$T_{\text{ion}}^{\text{outer}} = T_{\text{ion}}^{\text{inner}}$ and $\gamma_{\text{ion}}^{\text{outer}} = \gamma_{\text{ion}}^{\text{inner}} = 2$. As shown in Figure 3, the ELM target load difference is zero, i.e. the ELM energy load to inner and outer target is equal, when no net charge difference is measured. Since the energy load is equal when no net charge is measured, it is plausible to conclude that also the

particle fluxes due to an ELM are equal, i.e. $N_{ELM}^{outer} = N_{ELM}^{inner}$ is assumed. This number is approximated by calculating the ELM pedestal particle loss to find a typical values of $5 \cdot 10^{19}$ particles (i.e. this gives $N_{ELM}/C_{ELM} \approx -3$). Subtracting equation (2) from equation (1), dividing the result by $2k_B C_{ELM}$ gives then

$$\gamma_{ion} T_{ion} + \frac{3}{2} \cdot \gamma_{ele}^{inner} T_{ele}^{inner} - \frac{3}{2} \gamma_{ele}^{outer} T_{ele}^{outer} = \frac{E_{outer} - E_{inner}}{2k_B C_{ELM}} = 500eV.$$

A possible solutions of this equation is given e.g. by

$$\gamma_{ion} = 2, \gamma_{ele}^{inner} \approx \gamma_{ele}^{outer} \approx 2, T_{ele}^{inner} = 50eV, T_{ele}^{outer} = 100eV, T_{ion} = 400eV,$$

Although again not enough quantities of the above equation are measured, we can draw the important conclusion that in case $T_{ele}^{outer} \approx T_{ele}^{inner}$ is fulfilled during an ELM the corresponding value for T_{ion} must be much larger than the values for T_{ele}^{outer} , T_{ele}^{inner} . This result is well consistent to the finding of the ELM filament evolution in the SOL due to parallel losses [14]. Here only the two limits of attributing the net charge difference (1) fully towards the electrons and then (2) fully towards the ions have been briefly discussed. The same formalism has been repeated by attributing half of the net charge difference to the ions and half of it to the electrons. With the same numbers otherwise as stated above $T_{ion} = 700eV$ is found, therefore a value which exceeds the typical ion pedestal temperatures at AUG and therefore not realistic. Speculating on these findings, it seems that a net ion charge imbalance is causing the observed ELM target load differences.

4. COMPARISON OF ASDEX UPGRADE AND JET RESULTS

Figure 4 shows a comparison of JET and ASDEX Upgrade values of $E_{outer} + E_{inner}$ versus $E_{outer} - E_{inner}$ for ‘normal’ and ‘reversed’ field direction. For ASDEX Upgrade ELMs with target load energies from 2kJ to 20kJ (this number can be verified in Figure 4) it is observed that $-1/3 \times (E_{outer} + E_{inner}) \leq E_{outer} - E_{inner}$ for ‘normal’ and $0 \leq E_{outer} - E_{inner} \leq 2/3 \times (E_{outer} + E_{inner})$ for ‘reversed’ field discharges. Obviously there is an unidentified parameter varying the $E_{outer} + E_{inner}$ value for each given $E_{outer} + E_{inner}$ value; here comparison of $E_{outer} + E_{inner}$ values to the pre-ELM pedestal top values of T_e , electron density, collisionality and the normalized ELM pedestal loss size did not reveal a simple correlation. For JET the ELM target load energies cover values between 40kJ to 500kJ. For the ‘reversed’ field conditions more ELM energy is found to be deposited on the outer target and for ‘normal’ field cases more on the inner target identical to the findings for ASDEX Upgrade. The data base for ‘reversed’ field is otherwise very poor and therefore not further discussed here. For ‘normal’ field direction and again identical to ASDEX Upgrade the relation $-1/3 \times (E_{outer} - E_{inner}) \leq E_{outer} - E_{inner} \leq 0$ is found. For ELMs with target energies above 100kJ values only a comparable small variation of the $E_{outer} - E_{inner}$ values is observed and it is found that $E_{outer} - E_{inner} \approx -1/3 \times (E_{outer} - E_{inner})$. Note that the variation of the ELM target load data with target energies below 100kJ could also be introduced by the larger diagnostic error bars in JET. However, it seems plausible to speculate in that respect, that

the unidentified parameter plays a significant role for the comparable small ELMs in ASDEX and for low energy ELMs (<100kJ) in JET but not for large ELMs (>100kJ). Finally the corresponding value for E_{outer}/E_{inner} are calculated here for the largest ELM in JET for ‘normal’ field by

$$E_{outer} - E_{inner} \approx -1/3 \times (E_{outer} - E_{inner}) \Rightarrow \frac{E_{inner}}{E_{outer}} \approx 2$$

CONCLUSIONS

Several conclusions can be drawn from the presented observations. First, the finding that ELMs drive a larger fraction of energy to be deposited in ‘normal’ field direction towards the inner divertor is a true finding also for JET and not caused by diagnostically introduced artefacts as e.g. surface layers. Secondly, only a large difference between T_{ion} and T_{ele} is consistent to the findings presented in Section 3, which is consistent with the model of ELM filament energy evolution due to parallel losses [14]. In return the analysis in Section 3 suggests, that ion currents during the ELM, possibly caused by drifts in the SOL, are causing the observed energy/charge asymmetry. Thirdly, an unidentified parameter appears for all ELM data reported from ASDEX Upgrade (< 20kJ) and possibly for small ELMs at JET (<100kJ) which can causes values of $E_{outer} - E_{inner}$ to be close to zero. ‘ Note, that ‘no cases have been observed in ASDEX Upgrade upper single null or in JET DOC-L discharges where more energy was deposited to the outer target plate in ‘normal’ field or to the inner target plate in ‘reversed’ field. ‘Finally, for largest ELMs (>100kJ) at JET DOC-L discharges $E_{outer}/E_{inner} \approx 2$ is found. It may be of interest to note, that the latter value would be close to a ‘perfect’ value regarding the ITER divertor life time [3,6]. However, the *hidden* parameter must be identified before final conclusion can be given in that respect.

REFERENCES:

- [1] H.Zohm, Plasma Phys. Control. Fus. **38** (1996) 105.
- [2] D.J. Campbell, Phys. Plasmas **8** (2001) 2041.
- [3] G. Federici, Plasma Phys. Control. Fus. **45** (2003) 1523.
- [4] A.Kallenbach et al., Journal Nucl. Mater., **290-223** (2001) 639.
- [5] S.Jachmich, these proceedings
- [6] T. Eich *et al.* J. Nucl. Mat. **337-339** (2005) 669.
- [7] A.Herrmann, Plasma Phys. Control. Fus. **44** (2002) 883.
- [8] P.Andrew, Journal Nucl.Mater., **313-316** (2003) XXX
- [9] T.Eich et al., Plasma Phys. Control. Fus. **47** (2005) 815.
- [10] G.M. Staebler and F.L.Hinton, Nucl. Fus. **29** (1989) 1820.
- [11] C.Lasnier, Journal Nucl.Mater., **313-316** (2003) XXX
- [12] G.M.Staebler and F.L.Hinton, Nucl.Fusion **29** (1989) p.1820
- [13] R.A. Pitts, Nucl. Fus. **43** (2003) XXX.
- [14] W. Fundamenski, R.A. Pitts et al., Plasm.Phys. Contr. Fus. **48** (2006) 109.

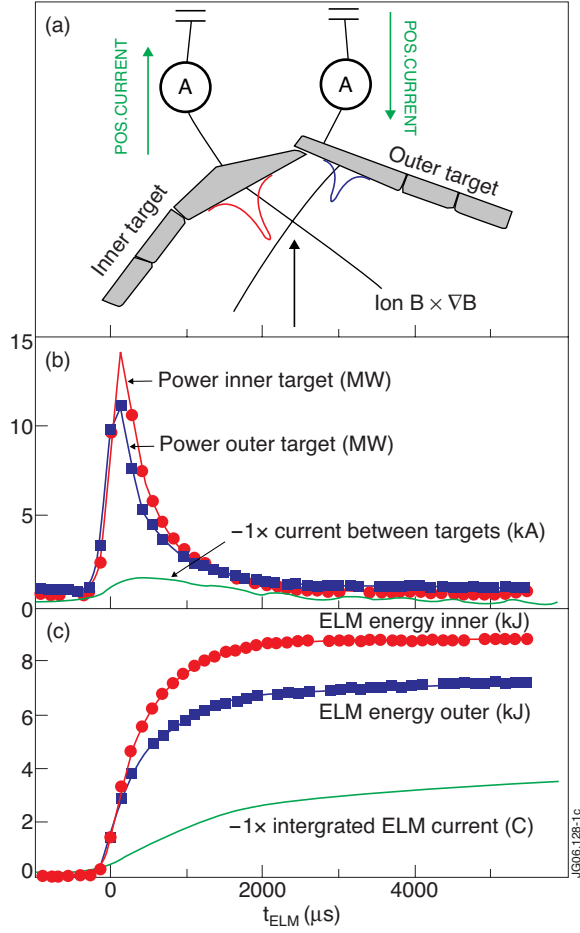


Figure 1: (a) Sketch of inner/outer ELM power load asymmetry and corresponding positive target current direction for ASDEX Upgrade Upper Single Null discharges. (b) Power load for inner (red) and outer (blue) target plates and target current evolution during type-I ELM in ASDEX Upgrade with 'normal' ion $B \times \nabla B$ drift direction pointing towards the active X-point for coherently averaged data of about 20 ELMs. (c) Time integrals of the values in (b) over ELM duration gives ELM deposited target energy inner E_{inner} (red), E_{outer} (blue) and C_{ELM} (green).

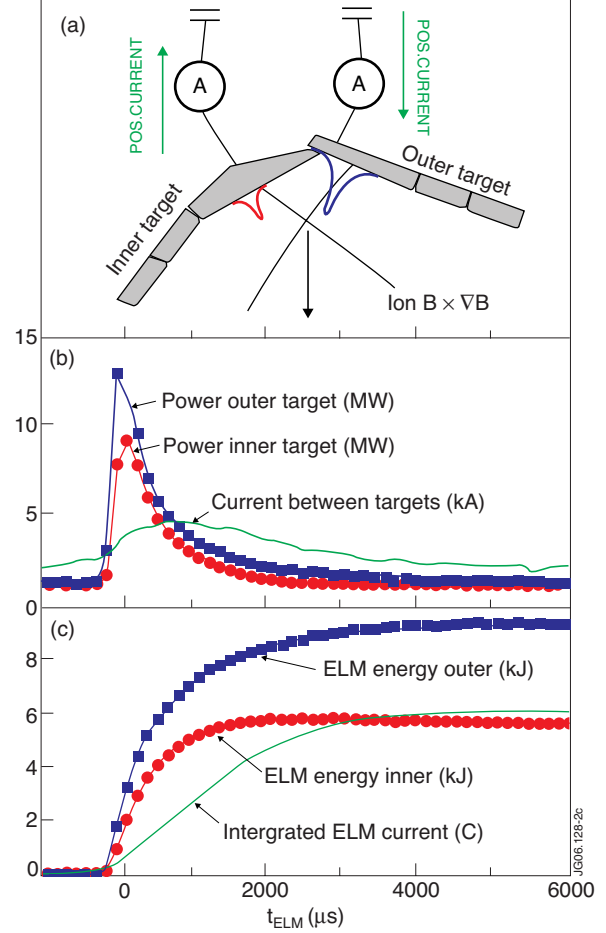


Figure 2: Same as in figure 1 with 'reversed' ion $B \times \nabla B$ drift direction pointing away from the active X-point.

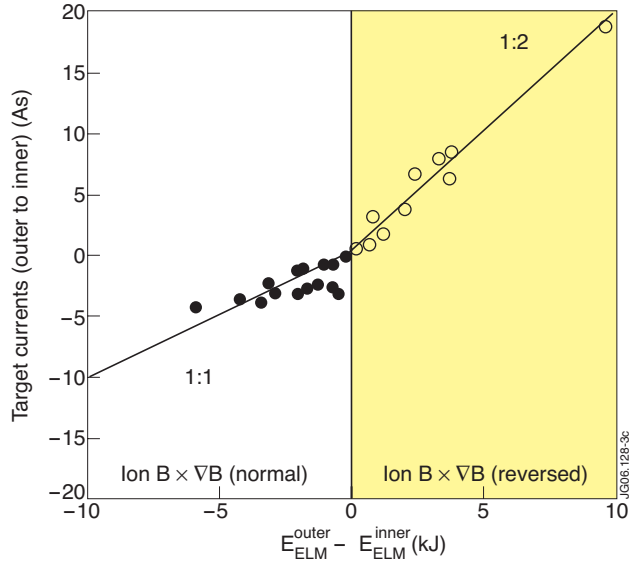


Figure 3: Correlation between the measured difference of ELM deposited energies towards inner and outer divertor target, $E_{outer} - E_{inner}$, with the time ELM related charge difference C_{ELM} . Note that both values, $E_{outer} - E_{inner}$ and C_{ELM} strictly change sign with field direction. Open symbols are 'reversed' field data and closed symbols 'normal field'.

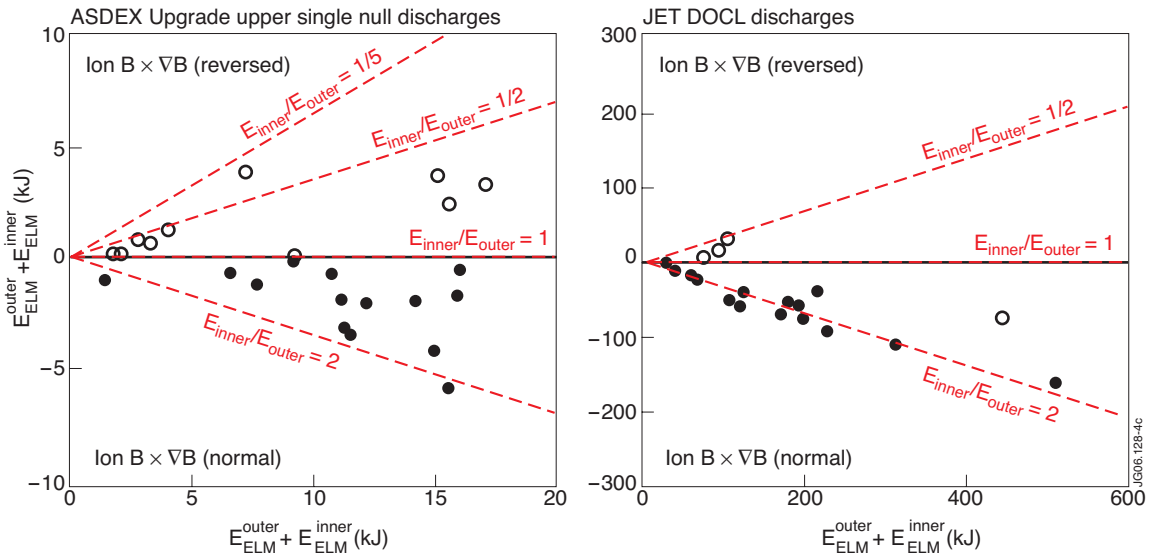


Figure 4: Correlation of the ELM deposited energy for both targets, $E_{outer} + E_{inner}$ with $E_{outer} - E_{inner}$ in ASDEX Upgrade and JET. In ASDEX Upgrade the data points are distributed due to an unidentified parameter in such a way, that with 'normal' field a range of $E_{outer}/E_{inner} = 1 - 2$ is found and with 'reversed' field a range of $E_{outer}/E_{inner} = 1/5 - 1$. (b) In JET the data points for large ELMs ($>100\text{kJ}$) in 'normal' field are close to $E_{outer}/E_{inner} = 2$. Open symbols are 'reversed' field data and closed symbols 'normal field'.